Fluidelastic Stability Analysis Using Unsteady Fluid Force Measurement of a Rotated Square Array Subjected to Two-phase Cross-flow

Sameh Darwish, Njuki Mureithi
2500 Chemin de Polytechnique, Montréal, QC H3T 1J4, Canada
sameh.darwish@polymtl.ca
njuki.mureithi@polymtl.ca
Minki Cho
Doosan Enerbility, Changwon-si, Gyeongnam, 51711, Republic of Korea
minki1.cho@doosan.com

The research findings presented in the literature confirmed that the rotated triangle array is inherently fluidelastically unstable in two-phase flow, especially in the transverse direction. On the other hand, recent work confirmed that the rotated square array is fluidelastically stable for all tested void fractions in two-phase flow, except for 97%. The quasi-steady analysis showed a significant reduction in damping for 97% void fraction compared to lower void fractions. The quasi-steady model, however, could not resolve the issue of the increase in tube bundle vibrations in the transverse direction for 97% void fraction. Hence, further analysis is required to deeply look into the array using the unsteady theory. In this work, the unsteady fluid forces were measure for a rotated square array with P/D=1.64. The advantage the unsteady theory has is taking into consideration the variation of the fluid force phase with reduced flow velocity. This is not encountered in the quasi-steady theory where the fluid force phase is always assumed to be constant. Unlike the quasi-static force measurements, the unsteady fluid dynamic force component and the vibration modes of the tubes are taken into account in the unsteady theory. The results of this work add a deeper understanding to the rotated square array dynamic behaviour. An array that showed a stable behaviour in two-phase flow. This study aimed in part to analyse the APR1400 steam generator tube bundle in single and two-phase cross-flow.

Keywords: Fluidelastic instability, Rotated square array, Two-phase flow, Steam generator

I. Introduction

Fluidelastic instability occurrence in nuclear reactor steam generators results in the reactor shutdown. The violent vibrations in the unstable tube bundle leads to vibration-induced tube wear and hence a leakage of the contaminated water inside the tubes. An extensive experimental effort was exerted to study all tube arrays in two-phase flow. However, theoretical modelling of this phenomenon still requires significant work. The first modelling approach was provided by Robert **[1]** using a jet switching mechanism. This approach didn't predict transverse fluidelastic instability. The unsteady model was developed by Tanaka and Takahara **[2, 3]** and Chen **[4]**. Later, Sawadogo and Mureithi **[5]** used a novel method to measure the unsteady fluid forces in a rotated triangular array in the transverse direction. A similar methodology was adopted by Shahriary et al. **[6]**, however, only quasi-static fluid forces were measured in the same array layout. Olala **[7, 8]** measured both quasi-static and unsteady fluid forces in the streamwise direction. The unsteady model was applied by Mureithi et al. **[9, 10]** who developed the time frequency analysis to calculate the tube displacement fluid force phase difference. Numerically, it was possible to incorporate the CFD solutions to perform similar analysis by Sadek et al. **[11]**. The numerical solution showed an acceptable accuracy, yet, still computationally expensive.

Very few research work measured experimentally the unsteady forces of tube arrays, and non yet did for the rotated square array. A full set of unsteady measurements was performed using the same test apparatus presented in Darwish et al. **[12].** In this study, the unsteady fluid forces, acting on a bundle of rigid tubes as a function of one tube displacement are measured in a rotated square array of P/D=1.64. The study is performed in both transverse and streamwise directions in water flow, and two phase flow at void fractions in the range 40%-97%. The experiments included the cross coupling fluid force measurements of the surrounding tubes that are instrumented using full bridge strain gauges. This study follows the fluidelastic instability experimental study presented in a previous study on the same array **[12, 13]**. These results are part of a detailed research work aimed to analyze the APR1400 nuclear reactor steam generator.

II. Experimental Apparatus

A two-phase flow test loop was designed to accommodate different test setups. The water flow circulates in the loop using a 7.5 HP centrifugal water pump from a large reservoir. A magnetic water flow meter (MAG500) is used to measure the water flow rate. Air is compressed and injected into the loop upstream the test section. Mixing air and water flows is appropriately done upstream the tube bundle using a two-layer mixer. The temperature of both water flow and air flow were monitored using calibrated thermocouples. The test loop is shown in Fig. 1.

Rigid tubes in the test section are arranged in 9 rows and 9 columns, with half tubes mounted on the side walls to reduce the wall effect. A central tube was designed and mounted on a force sensor, connected to a linear motor. The motor is controlled by an Aries smart AR-04CE servo-drive. The advantage in using this motor generating a direct linear motion, enhanced by using a linear magnetic encoder with ±30 μm accuracy. The neighboring tubes are made of Plexiglas and instrumented with strain gauges to measure the cross-coupling fluid forces, see Fig. 2. Measuring the cross coupling fluid forces will be utilized in future work by using the unsteady model to provide further detailed study of the array. For brevity, in this paper only central tube results are presented.

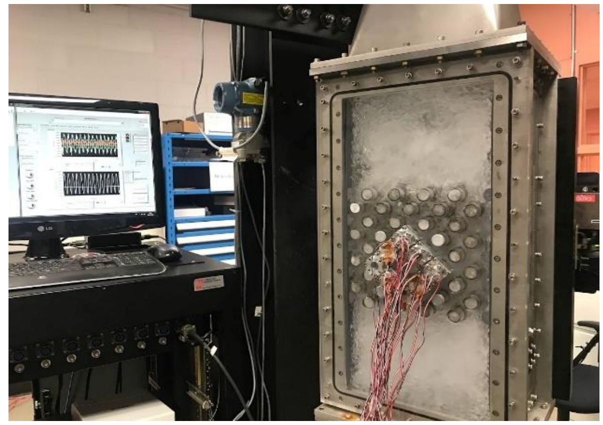

Fig. 1. Experimental Setup

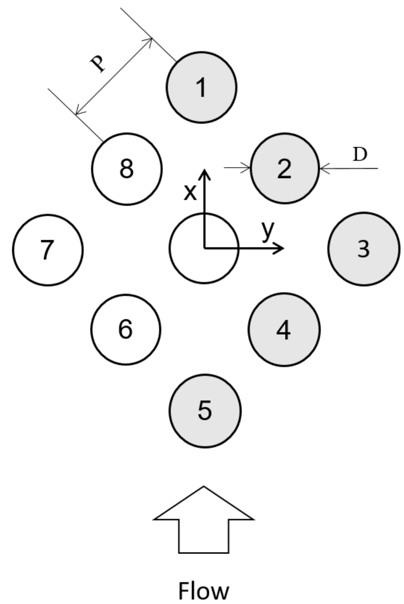

Fig. 2. Schematic of the array layout and neighbouring tubes numbers.

III. Mathematical Formulation

The method employed in the analysis of the measured unsteady fluid forces is outlined below. When a harmonic motion of the form $x(t) = x_o e^{i\omega t}$ is applied to a tube in a rigid tube bundle, the fluid force per unit length on the tube may be expressed as [9]

$$F = [\omega^2 (m + 2\rho R^2 c_{ma}) + i\omega\rho V_p R c_{da} + \frac{\rho U^2}{2} c_s] x(t) \quad (1)$$

where, R is the tube radius, V_p flow velocity, ρ flow density, m is the tube mass per unit length, D is tube diameter c_{ma}, c_{da} and c_s are are the fluid added mass, damping and stiffness coefficients, respectively. By defining a force/displacement transfer function

$$H_{Fx} = \frac{F}{x_o e^{i\omega t}} \tag{2}$$

Equating the real and imaginary parts of this transfer function to the corresponding components of the fluid force yields

$$Re[H_{Fx}] = \omega^2 (m + 2\rho R^2 c_{ma}) + \frac{\rho U^2}{2} c_s \tag{3}$$

$$Im[H_{Fx}] = \omega \rho V_p R c_{da} \tag{4}$$

The fluid stiffness together with the added mass component is therefore given by

$$F_{s,ma} = [\omega^2 (m + 2\rho R^2 c_{ma}) + \frac{\rho V_p{}^2}{2} c_s] x_o - m\omega^2 x_o \tag{5}$$

where the last term is related to tube inertia, and determined by performing tests in air. The damping force then will be

$$F_{da} = Im[H_{Fx}] x_o \tag{6}$$

The force coefficient magnitude will be

$$c_f = \frac{(F_{s,ma}^2 + (Im[H_{Fx}] x_o)^2)^{0.5}}{0.5 \rho V_p{}^2 x_o} \tag{7}$$

The phase angle between the fluid force and tube displacement then becomes

$$\phi_f = tan^{-1}[\frac{Im[H_{Fx}] x_o}{F_{s,ma}}] \tag{8}$$

Then the damping coefficient becomes

$$c_f = \frac{-Im[H_{Fx}]}{\omega} \tag{9}$$

while the total damping factor is given by

$$\zeta = \frac{-Im[H_{Fx}]}{2(m + m_a)\omega^2} \tag{10}$$

Using previously measured quasi-static forces for this rotated square array, the time delay, τ, can be estimated such that [5]

$$\tau = -\frac{1}{\omega} \sin^{-1} (\frac{\omega D}{C_{L,Y/D}} [\frac{C_{Do}}{V_p} + \frac{C_{da}}{V}]) \tag{11}$$

The homogeneous air-water flow void fraction, β, is calculated as a ratio between air flow rate to flow mixture total flow rate

$$\beta = \frac{Q_a}{Q_a + Q_w} \tag{12}$$

where, Q_a and Q_w is the volumetric flow rate of air and water, respectively. The homogeneous density, ρ, is defined using the homogeneous void fraction as

$$\rho = \beta \rho_a + \beta (1 - \rho_w) \tag{13}$$

In this test setup, only the central tube is displaced. The surrounding tubes force derivatives can be deduced, considering the neighboring tube relative location to the central tube. The unsteady forces were acquired for multiple tube vibration frequencies for 6-20 Hz. Flow velocity variation was also necessary to have wide range of the flow reduced velocity, V/fD.

IV. Results

As this array was proven to be fluidelastically stable in the streamwise direction, results here focus mainly on the transverse direction that is known to be more unstable in all tube arrays. The unsteady fluid force phase and magnitude are presented in Fig. 3 for forced oscillations for the transverse direction, for 40%, 90% and 97% void fraction two-phase flows. An approximate analytical curve was fitted to the exported data to show the trend of the fluid phase and force coefficient with reduced flow velocity, V_p / fD. The phase angle is seen to decrease with the flow reduced velocity. This is, however, different in the 97% void fraction case in the transverse direction, where the phase is seen to gradually increase, reaching a maximum value near $V_p / fD = 20$, followed by a decrease at high velocities.

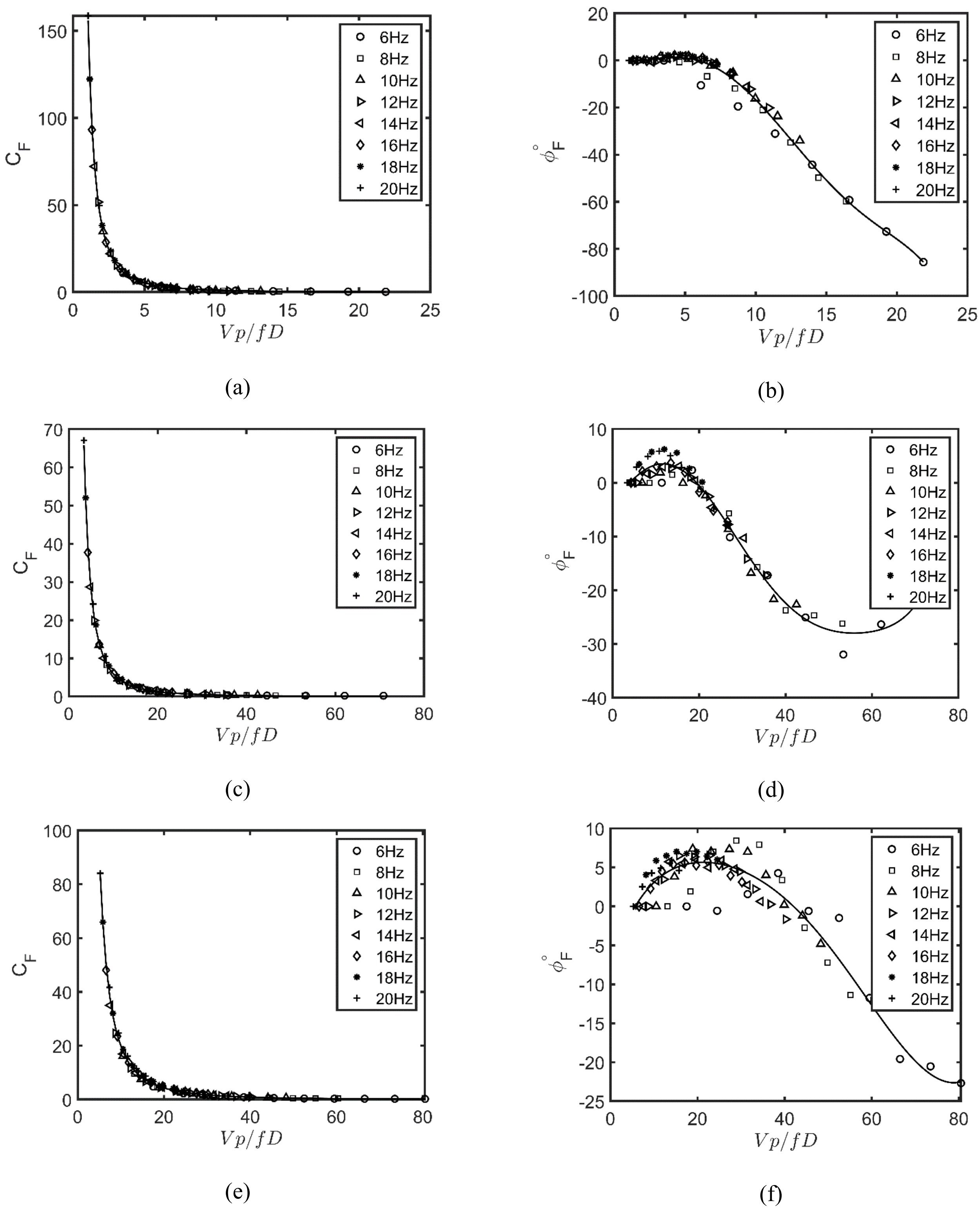

Fig. 3. Force coefficient and phase difference for the central tube for 6-20 Hz excitation frequencies in the transverse direction for: (a,b) 40%, (c,d) 90% and (e,f) 97%.

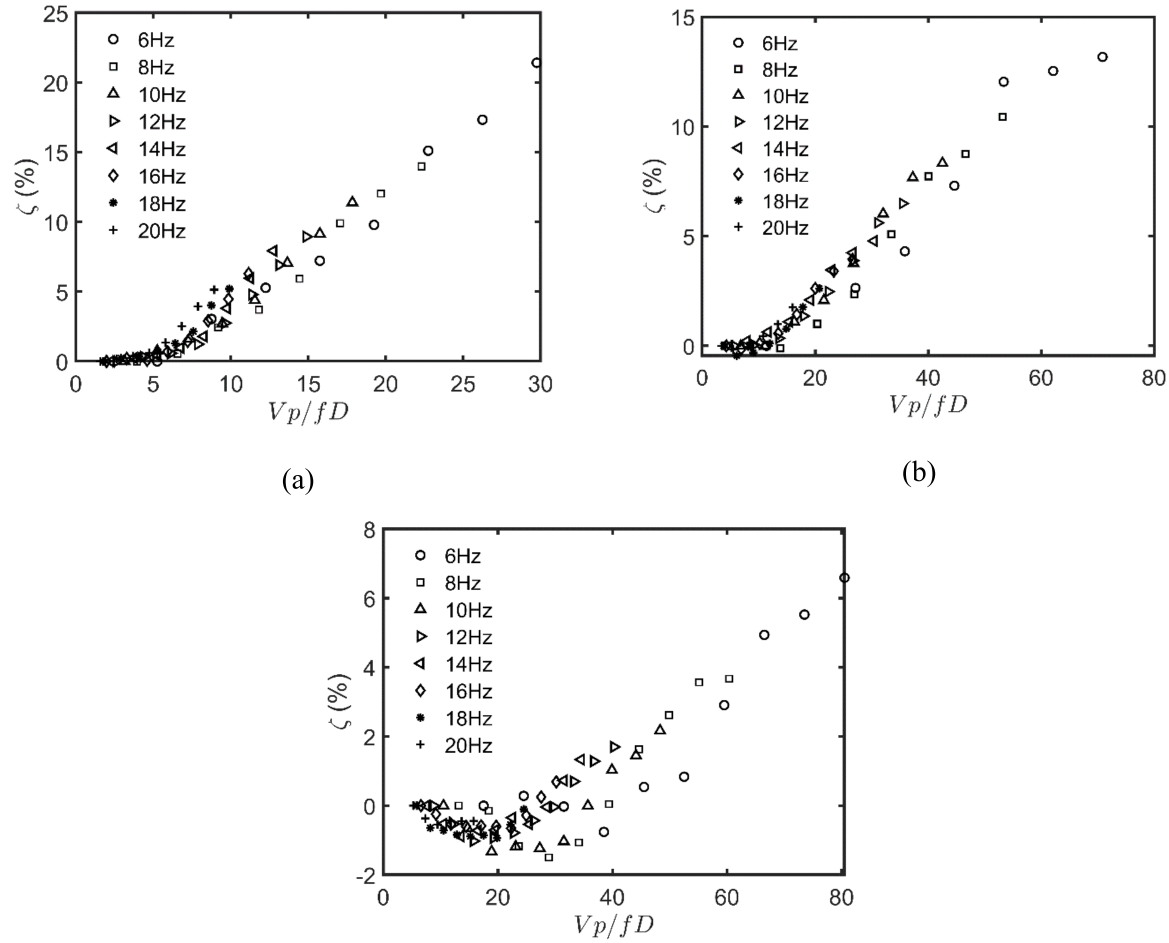

(a) (b) (c)

Fig. 4. Damping variation of central tube in the transverse direction in: (a) 60%, (b) 90% and (c) 97% void fractions

This is found to clearly occur for 97% void fraction, and only in the transverse direction. The range of the flow velocity where the fluid phase is positive indicates a reduction in fluid damping. Fig. 4 presents the calculated damping from the unsteady model for 60%, 90%, and 97% void fractions. This is the net (velocity dependent) damping. Compared to the 60% and 90% void fractions, it is clear that the net fluid damping decreases, and becomes negative in the range $7 \leq V_p / fD \leq 30$ for 97% void fraction. This has significant implications for the tube array subjected to two-phase flow of 97% void fraction. The reduction in the total damping of the flexible tube would be expected to lead to an increase in tube vibrations and fluidelastic instability in this velocity range. Fig. 5 shows the single flexible tube vibration in the transverse direction for the 97% void fraction. The foregoing effect is precisely observed in the tests. This effect may be amplified for a fully flexible array with multiple flexible tubes. Indeed the results here confirm the existence of the instability we term 'velocity limited' instability which, differs from the classical fluidelastic instability which shows no restabilization for high flow velocities.

In water flow, it was seen that a strong lock-in effect was uncovered in this array due to vortex shedding excitation [13]. In comparison to other array geometries, much larger resonance vibration amplitudes was found in this array in water flow. The damping in water flow was also calculated and shown in Fig. 6 along with the single tube vibration in the transverse direction. This result confirm the lock-in with the formed vortex shedding with a potential of fluidelastic instability to occur. Taking into consideration that the damping shown in Fig. 6 is the total fluid damping, we realize that adding the structural damping and the fluid damping will result in higher total damping over the same range of flow velocity. However, the reduction in total damping shown in the results suggest that fluidelastic instability could potentially occur for the single flexible tube. This explanation is supported with the fact that when multiple flexible tubes and examined, instability was confirmed using the quasi-steady model [12]. In Darwish et al. [13], using a splitter plate downstream the flexible tube suppressed the lock-in, which indicated that no fluidelastic instability existed in the single flexible tube case. However, it is still possible to see fluidelastic forces to cause a minor reduction in total damping, followed by violent vibrations resulting from the lock-in.

The time delay was estimated from Eq. 11, however, the formula developed so far limits the range of flow velocity and vibration frequencies that can be used in the calculations. Here, the time delay could be extracted from the water flow tests. Fig. 7 shows the time delay parameter, μ, calculated from the time delay ($\tau = \mu D / V_p$). The value is in the range of 1.6. This also confirms that the assumption of $\mu \approx 1$ is valid in this array in water flow.

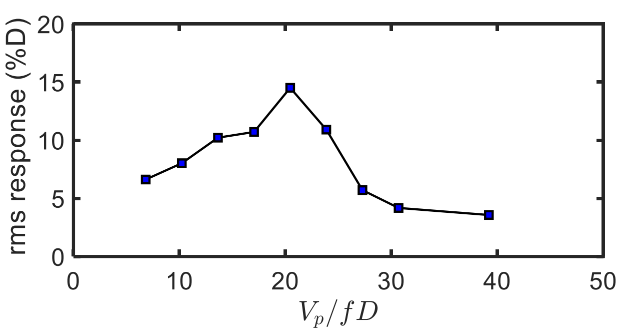

Fig. 5. Single flexible tube vibrations in the transverse direction for β=97%.

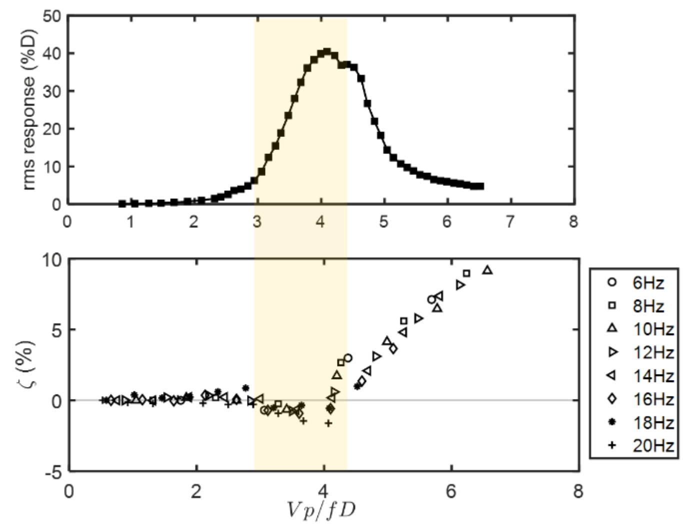

Fig. 6. Predicted Lock-in range from the damping estimation in water flow in comparison with the experimental results.

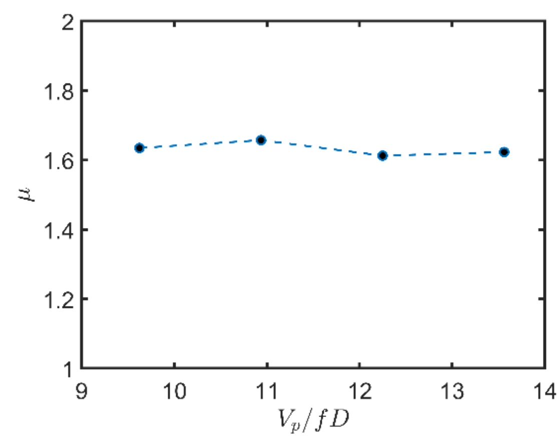

Fig. 7. Time delay constant exported from water flow fluid forces.

V. Conclusions

The results of this study have contributes to the understanding of the stability of the APR1400 nuclear reactor steam generator. After experimentally studying the rotated square array in two-phase flow, the partially explained the condition of "apparent transverse instability" that was found at the 97% void fraction vibration tests was still questionable. At the same time, it became clear that the limitations of the quasi-steady model made it impossible to fully explain the apparent instability. Further investigation was therefore done via unsteady force measurements which were conducted for the same flow conditions as the stability tests. The phase angle between the tube motion and the fluid forces was extracted for a wide range of reduced flow velocities. This is accomplished by varying both the flow velocity and the tube dynamic excitation frequency. The phase angle was seen in the 97% void fraction to initially increase at low reduced flow velocity, and then decrease at higher velocities. This translates into an initial decrease in the flow-induced damping thus leading to instability followed by an increase in damping and consequently tube restabilization for high flow velocities. This directly correlates with the observations made in the dynamics tests and this explains the 'apparent instability' described above. Also the time delay parameter was extracted in water flow, and was found to be around 1.6 in the transverse direction.

Acknowledgments

This work is funded by Doosan Enerbility. The authors also acknowledge the technical support of Nour Aimène at Polytechnique Montreal, and wish to thank A. Hadji and H.P. Pham for their effort in the project.

Nomenclature

P/D	Array pitch to diameter ratio
V_p	Flow pitch velocity
c_{ma}, c_{da}, c_s	Fluid added mass, added damping, and added stiffness coefficients, respectively
c_f	Damping coefficient
$C_{L,Y/D}$	Derivative of lift coefficient with respect to dimensionless displacement in the y direction.
C_{Do}	Coefficient of drag force at the central position
F_{da}	Damping force
R	Tube radius
m, m_a	Tube mass, and added mass per unit length
H_{Fx}	Transfer function
β	Two-phase flow void fraction
ζ, ζ_s	Damping ratio, structural damping ratio
μ	Time delay parameter
Φ_f	Phase angle
ω	Vibration frequency

References

1. Roberts, B.W., *Low frequency, self-excited vibration in a row of circular cylinders mounted in an airstream*, 1962, University of Cambridge, Eng.

2. Tanaka, H. and S. Takahara. *Unsteady fluid dynamic force on tube bundle and its dynamic effect on vibration*. in *ASME century 2 emerging technology conference*. 1980.

3. Tanaka, H. and S. Takahara, *Fluid elastic vibration of tube array in cross flow.* Journal of sound and vibration, 1981. **77**(1): p. 19-37.

4. Chen, S., *A general theory for dynamic instability of tube arrays in crossflow.* Journal of Fluids and Structures, 1987. **1**: p. 35-53.

5. Sawadogo, T. and N. Mureithi, *Fluidelastic instability study in a rotated triangular tube array subject to two-phase cross-flow. Part I: Fluid force measurements and time delay extraction.* Journal of Fluids and Structures, 2014. **49**: p. 1-15.

6. Shahriary, S., N.W. Mureithi, and M.J. Pettigrew. *Quasi-static forces and stability analysis in a triangular tube bundle subjected to two-phase cross-flow*. in *ASME Pressure Vessels and Piping Conference*. 2007.

7. Olala, S. and N.W. Mureithi, *Prediction of streamwise fluidelastic instability of a tube array in two-phase flow and effect of frequency detuning.* Journal of Pressure Vessel Technology, 2017. **139**(3): p. 031301.

8. Olala, S.O., *Streamwise fluidelastic instability of tube arrays subjected to two-phase flow*2016: Ecole Polytechnique, Montreal (Canada).

9. Mureithi, N., et al., *Dynamics of an in-line tube array subjected to steam–water cross-flow. Part II: Unteady fluid forces.* Journal of fluids and structures, 2002. **16**(2): p. 137-152.

10. Sawadogo, T. and N. Mureithi, *Fluidelastic instability study on a rotated triangular tube array subject to two-phase cross-flow. Part II:*

Experimental tests and comparison with theoretical results. Journal of Fluids and Structures, 2014. **49**: p. 16-28.

11. Sadek, O., A. Mohany, and M. Hassan, *Numerical investigation of the cross flow fluidelastic forces of two-phase flow in tube bundle.* Journal of Fluids and Structures, 2018. **79**: p. 171-186.

12. Darwish, S., N. Mureithi, and M. Cho, *Stability behaviour of a rotated square tube array subjected to two-phase cross-flow.* Nuclear Engineering and Design, 2023. **406**: p. 112235.

13. Darwish, S., et al., *Flow-induced vibrations of a rotated square tube array subjected to single-phase cross-flow.* Journal of Pressure Vessel Technology, 2022. **144**(4): p. 041405.